Supplementary Information

Dual functional turn-on non-toxic chemosensor for highly selective and sensitive visual detection of Mg^{2+} and Zn^{2+}: solvent-controlled recognition effect and bio-imaging application

Yang Wang[a], Zhi-Gang Wang[a], Xue-Qing Song[a], Qian Chen[a], He Tian[a], Cheng-Zhi Xie*[a,b], Qing-Zhong Li[c], Jing-Yuan Xu*[a]

[a] *Department of Chemical Biology and Tianjin Key Laboratory on Technologies Enabling Development of Clinical Therapeutics and Diagnostics, School of Pharmacy, Tianjin Medical University, Tianjin 300070, P. R. China.*

[b] *Key Laboratory of Advanced Energy Materials Chemistry (Ministry of Education), Nankai University, Tianjin 300071, P.R. China.*

[c] *The Laboratory of Theoretical and Computational Chemistry, School of Chemistry and Chemical Engineering, Yantai University,Yantai 264005, P.R. China.*

* *E-mail: xujingyuan@tmu.edu.cn, xiechengzhi@tmu.edu.cn*

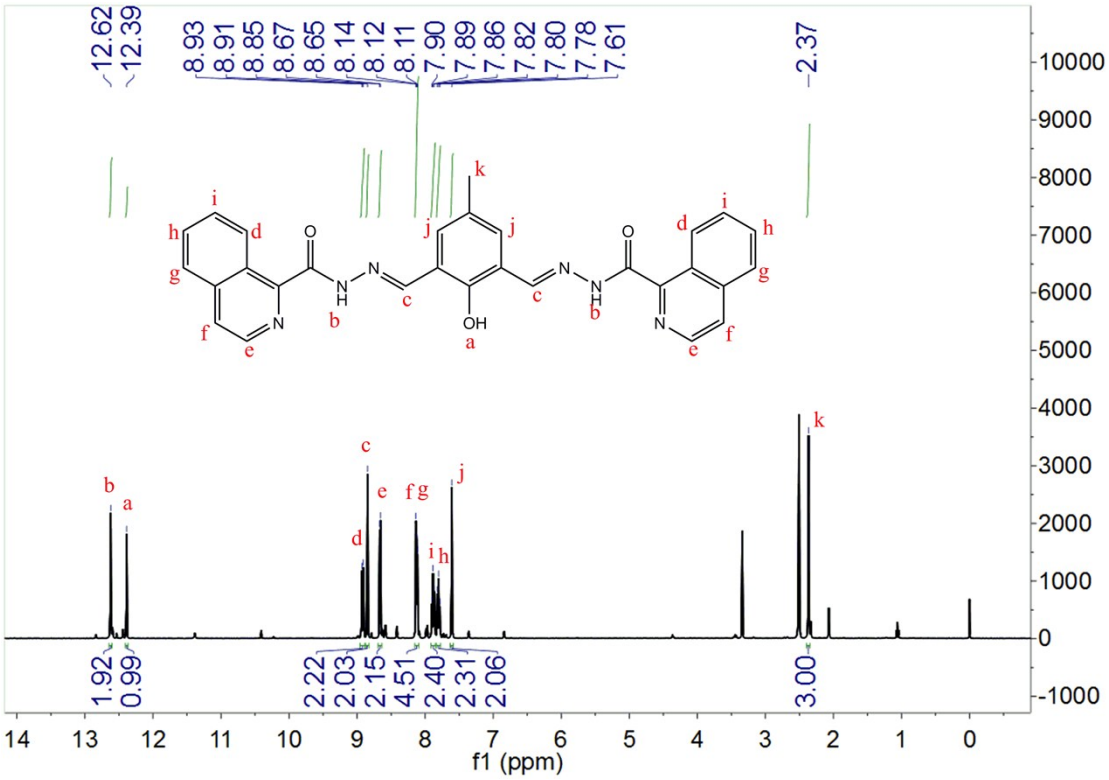

Figure S1. ^{1}H NMR of HL in DMSO-d_6

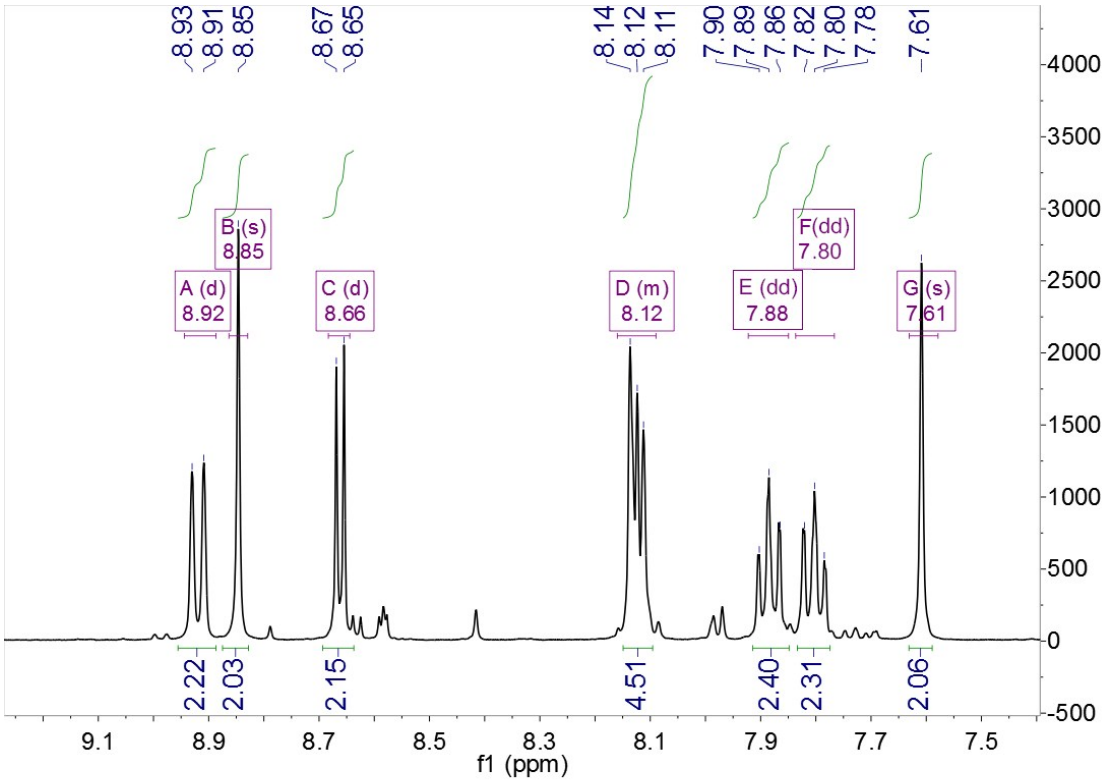

^{1}H NMR (400 MHz, DMSO) δ 8.92 (d, J = 8.5 Hz, 2H), 8.85 (s, 2H), 8.66 (d, J = 5.6 Hz, 2H), 8.09–8.15 (m, 4H), 7.88 (dd, J = 7.5, 7.2 Hz, 2H), 7.80 (dd, J = 7.2, 7.5 Hz, 2H), 7.61 (s, 2H).

Figure S2. Expanded ^{1}H NMR of HL in DMSO-d_6

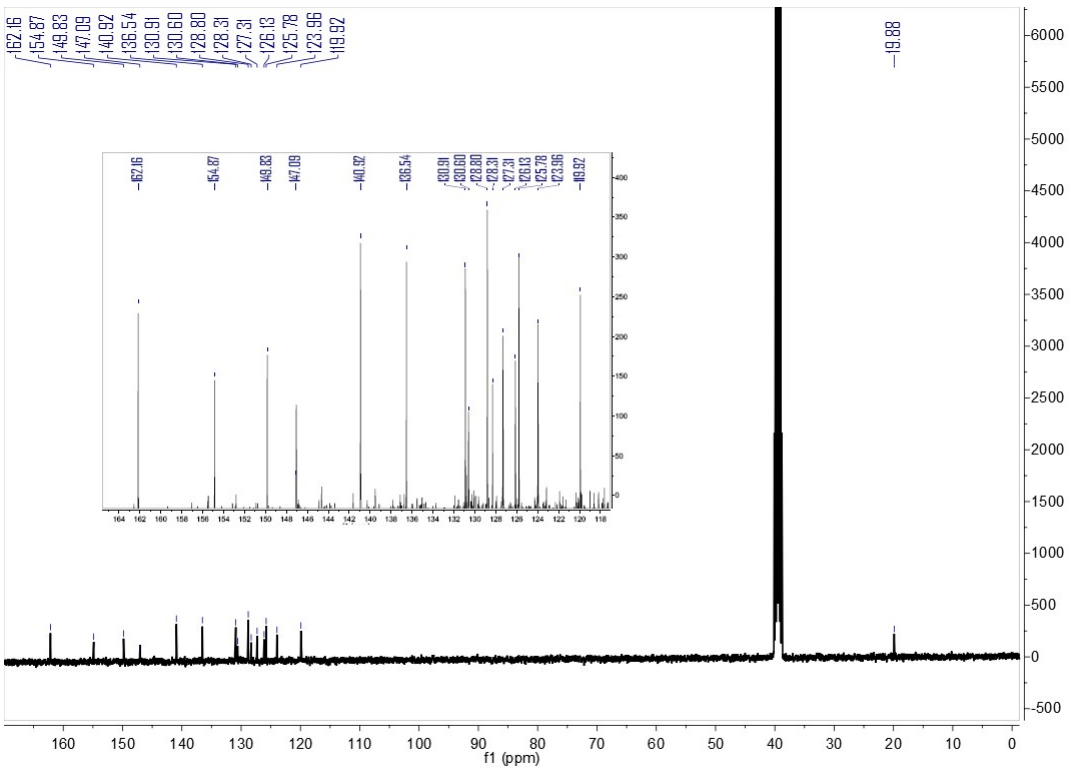

Figure S3. ^{13}C NMR of HL in DMSO-d_6

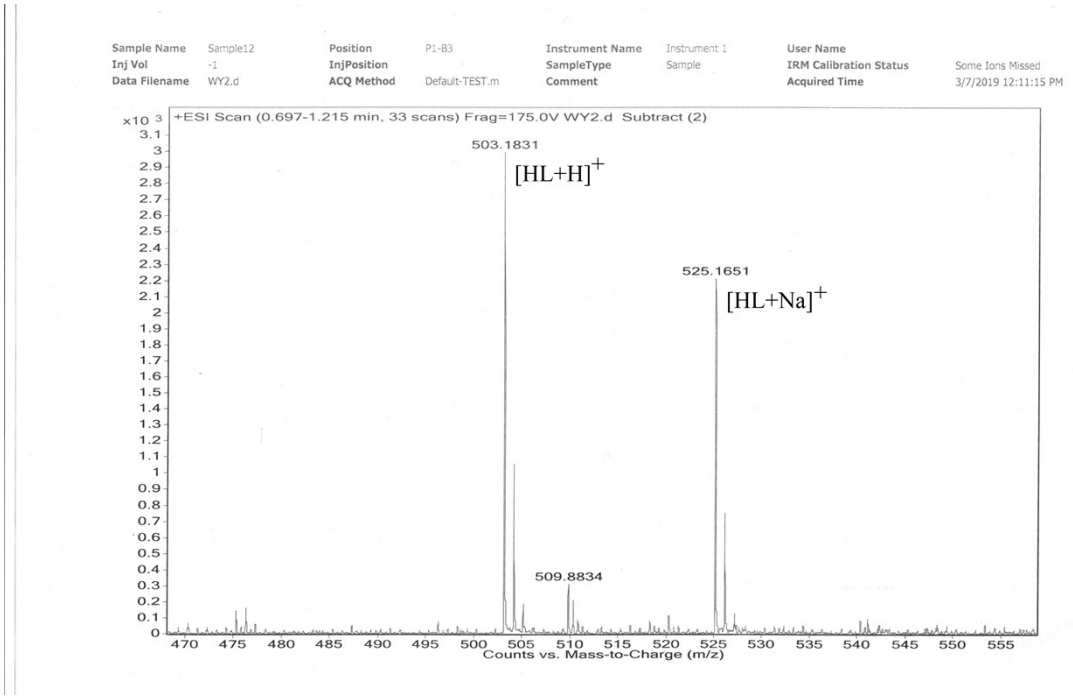

Figure S4. ESI-MS spectrum of HL

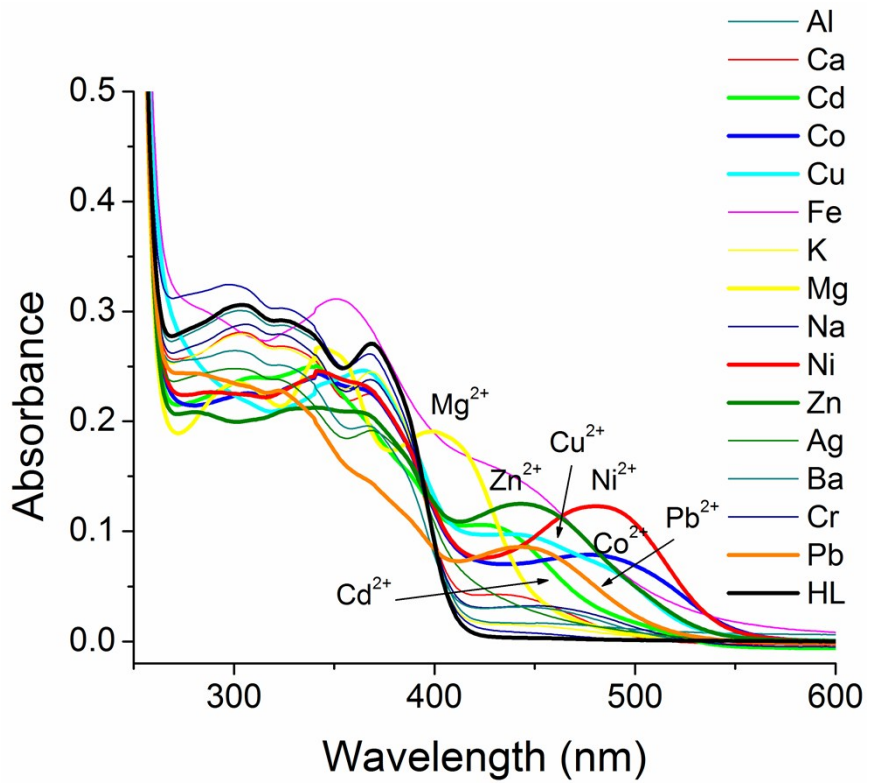

Figure S5. Absorption spectra changes of HL (10 μM) with various metal ions (1 eq.) in acetonitrile.

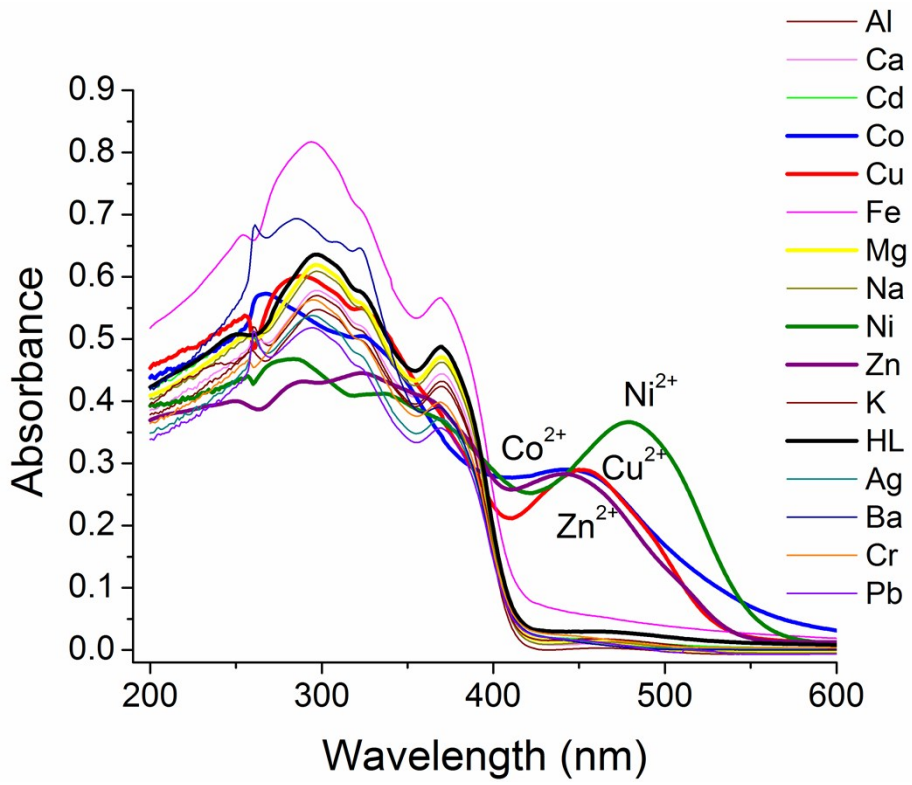

Figure S6. Absorption spectra changes of HL (20 μM) with various metal ions (1 eq.) in 9:1 *v/v* DMF:H_2O buffer solution (pH = 7.4).

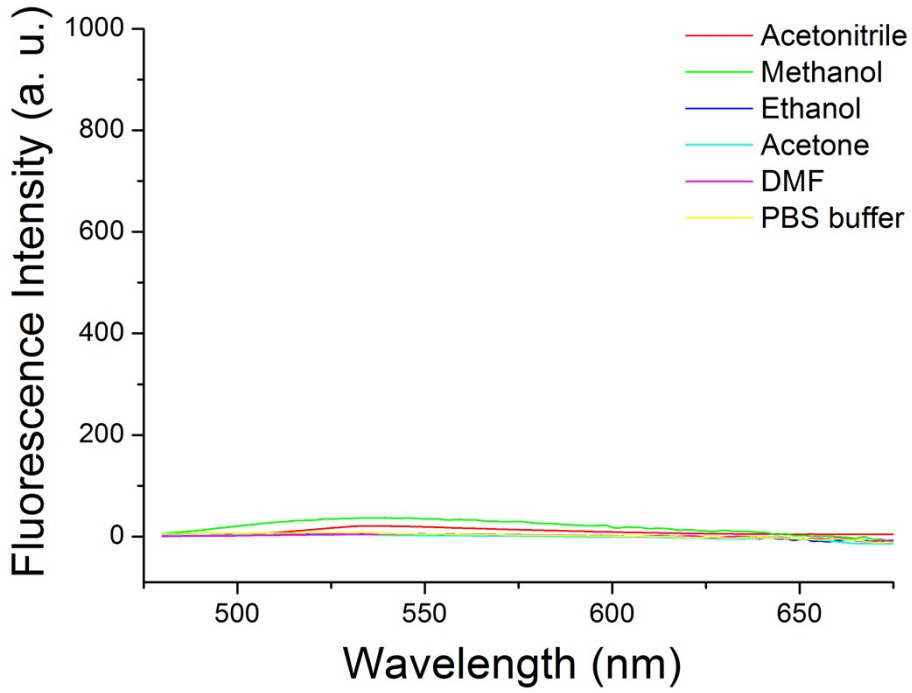

Figure S7. Fluorescence spectra of HL (10 μM) in different solvents (λ_{ex} = 350 nm).

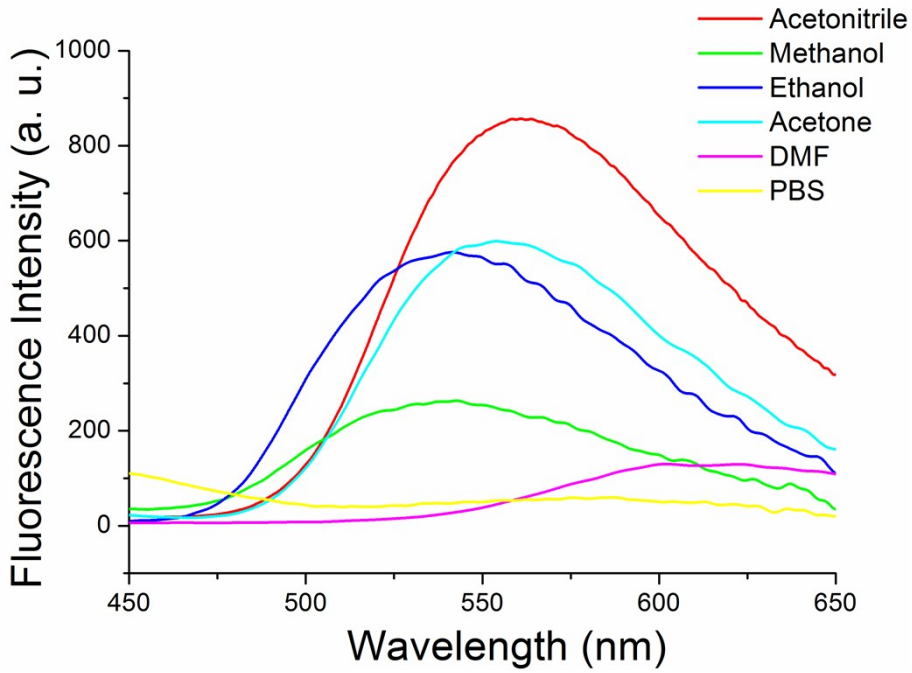

Figure S8. Fluorescence spectra of HL (10 μM) in presence of $Mg(NO_3)_2$ (10 μM) in different solvents (λ_{ex} = 350 nm).

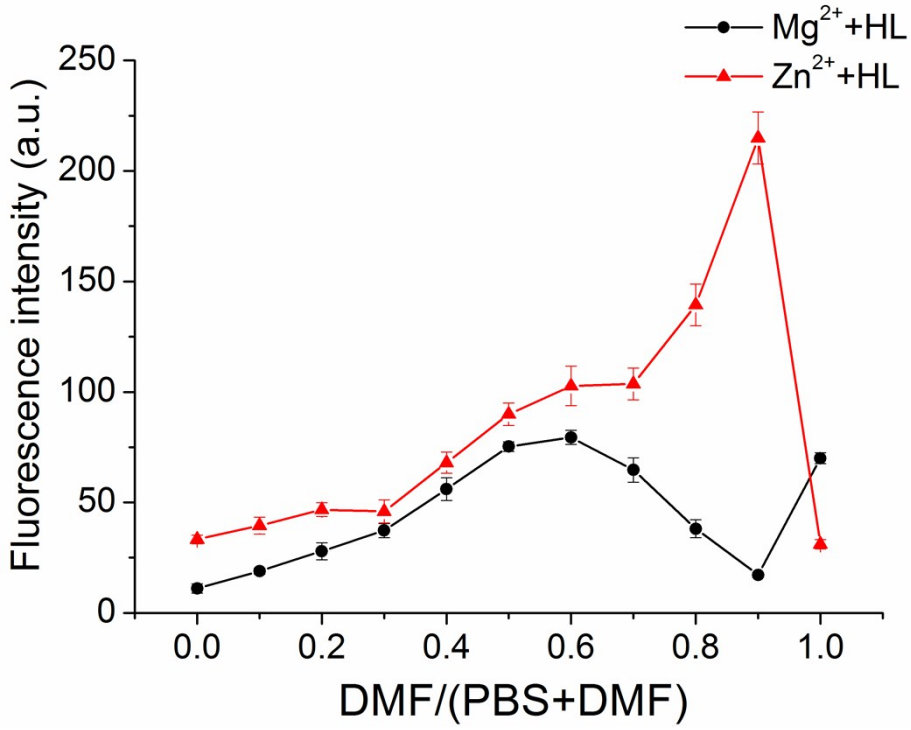

Figure S9. Fluorescence intensity curve of Mg^{2+}+HL and Zn^{2+}+HL (concentrations of HL and metal ions are all 20.0 μM) in different ratios of DMF/PBS solution (λ_{ex} = 460 nm).

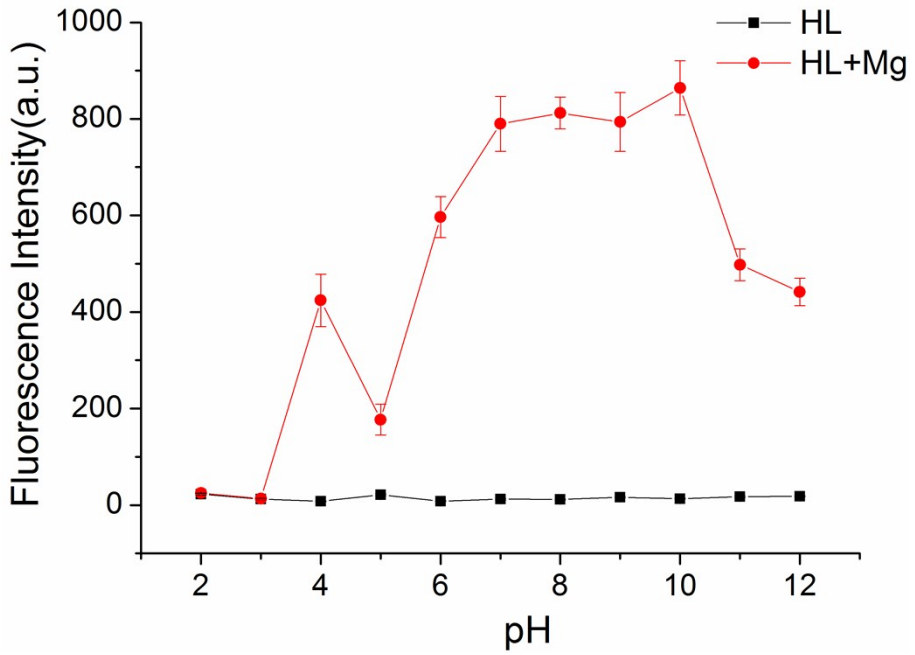

Figure S10. Effect of pH variation on Mg^{2+} sensitivity (concentrations of HL and $Mg(NO_3)_2$ are both 10.0 μM). Error bars were obtained from three measurements.

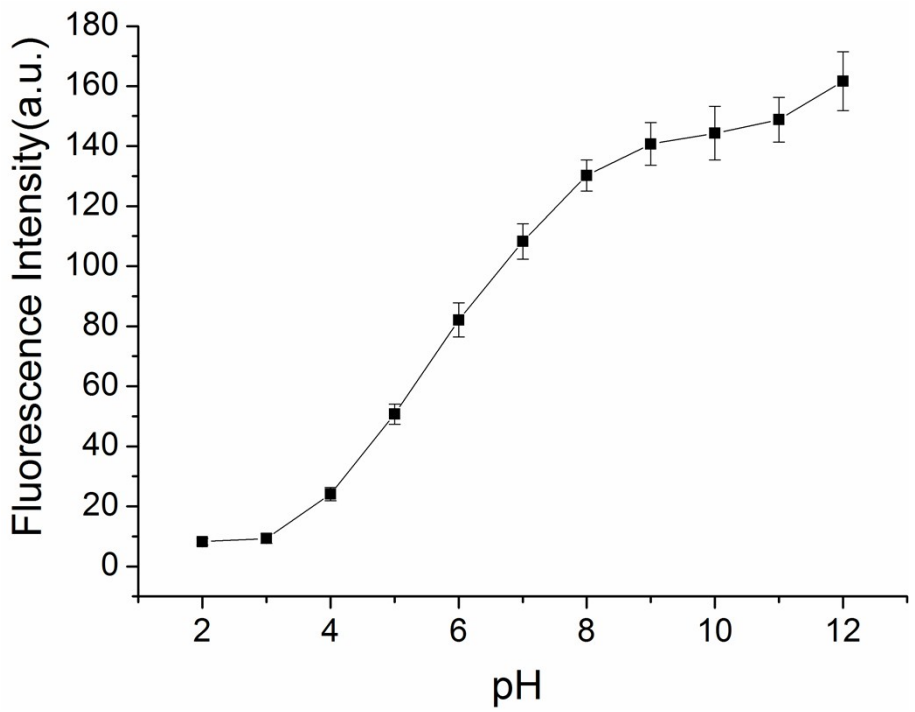

Figure S11. Effect of pH variation on Zn^{2+} sensitivity (concentrations of HL and $Zn(NO_3)_2$ are both 10.0 μM). Error bars were obtained from three measurements.

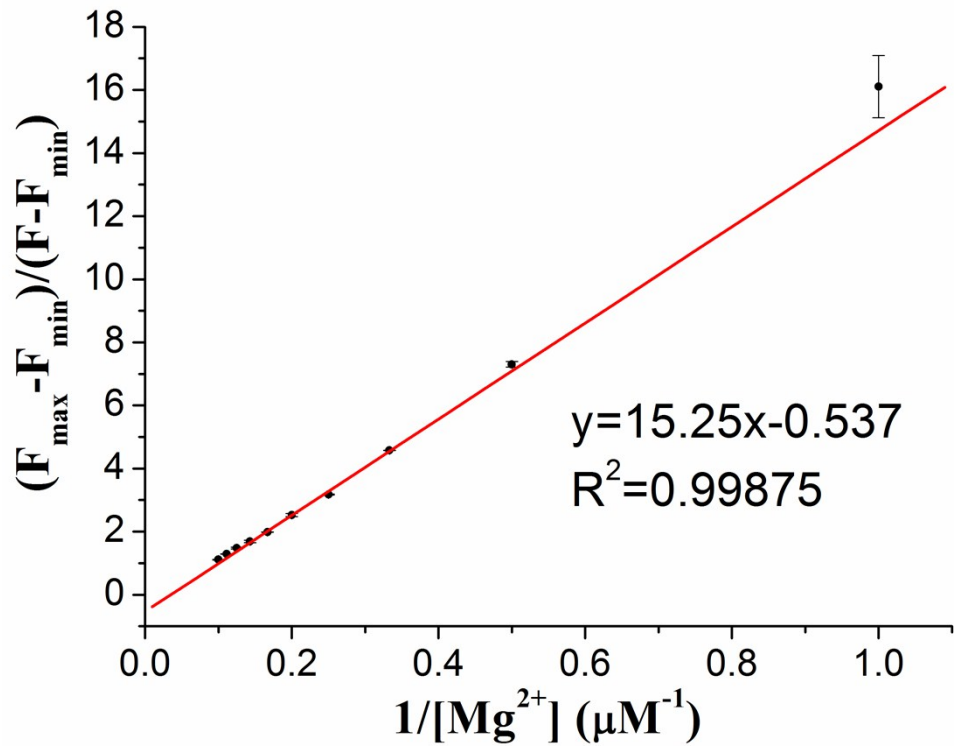

Figure S12. Modified Benesi-Hildebrand analysis of the emission changes for the complexation between HL and Mg^{2+}. Error bars were obtained from three measurements

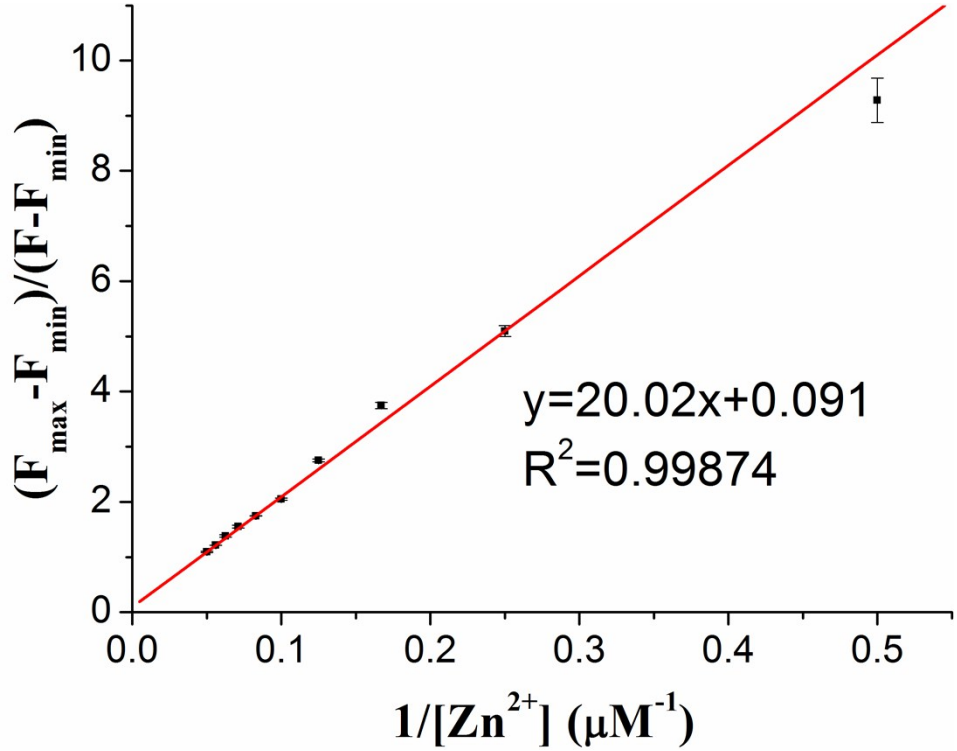

Figure S13. Modified Benesi-Hildebrand analysis of the emission changes for the complexation between HL and Zn^{2+}.

Determination of detection limit:

The detection limits (DL) for Mg^{2+} and Zn^{2+} were determined based on the fluorescence titration. The fluorescence emission spectrum of HL was measured 10 times, and the standard deviation (σ) of the blank measurement was achieved. DL of receptor HL for Mg^{2+} and Zn^{2+} were calculated using the following equation: DL = $3\sigma/\kappa$, where σ represents the standard deviation of blank controls, κ represent the slope of relative intensity changes (I/I_0-1) versus [M^{2+}] (M = Mg, Zn). I_0 is the emission intensity of HL at λ = 350 nm or 460 nm, I is the observed emission intensity at that particular wavelength in the presence of a certain concentration of the metal ion [M^{2+}]. To gain the slope, the fluorescence emissions at 350 nm and 460 nm were plotted as concentration of Mg^{2+} and Zn^{2+} respectively from their corresponding titration spectra. For Mg^{2+}, from the graph we get slope $\kappa = 8.84\times10^6$, and σ value is 0.0874 (Fig. S13).Thus using the formula we get the DL = 2.97×10^{-8} M. For Zn^{2+}, from the graph we get slope $\kappa = 5.00\times10^5$, and σ value is 0.0512 (Fig. S14).Thus using the formula we get the DL = 3.07×10^{-7} M.

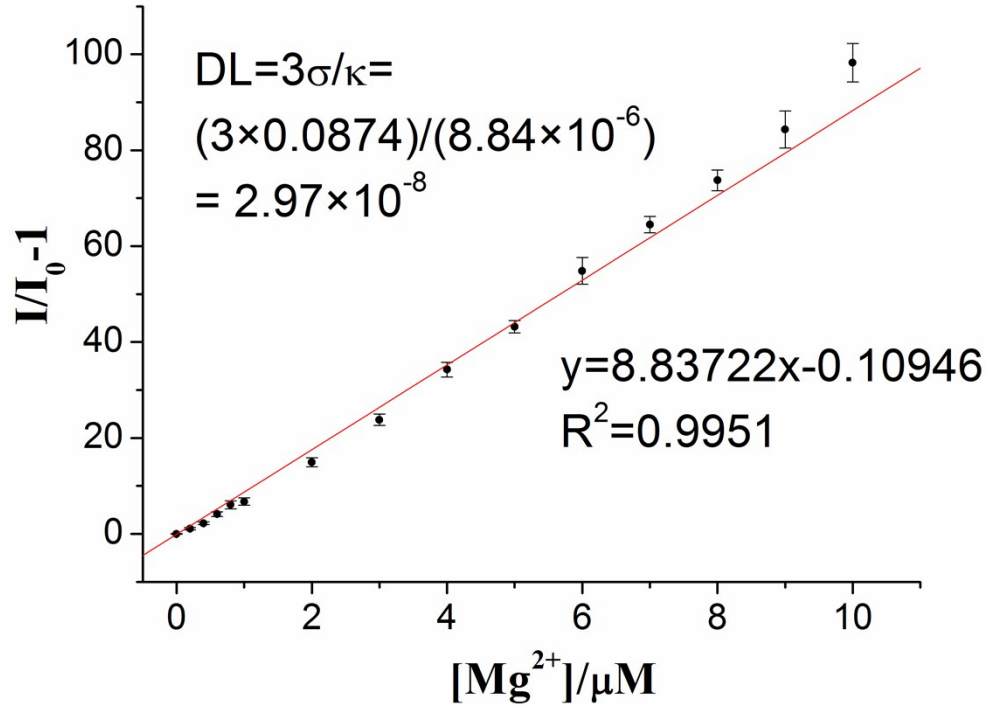

Figure S14. Linear fit equation for detection limit calculation of HL with Mg^{2+} in acetonitrile solution. The detection limit was determined to be 2.97×10^{-8} M based on relative fluorescence intensity changes versus $[Mg^{2+}]$.

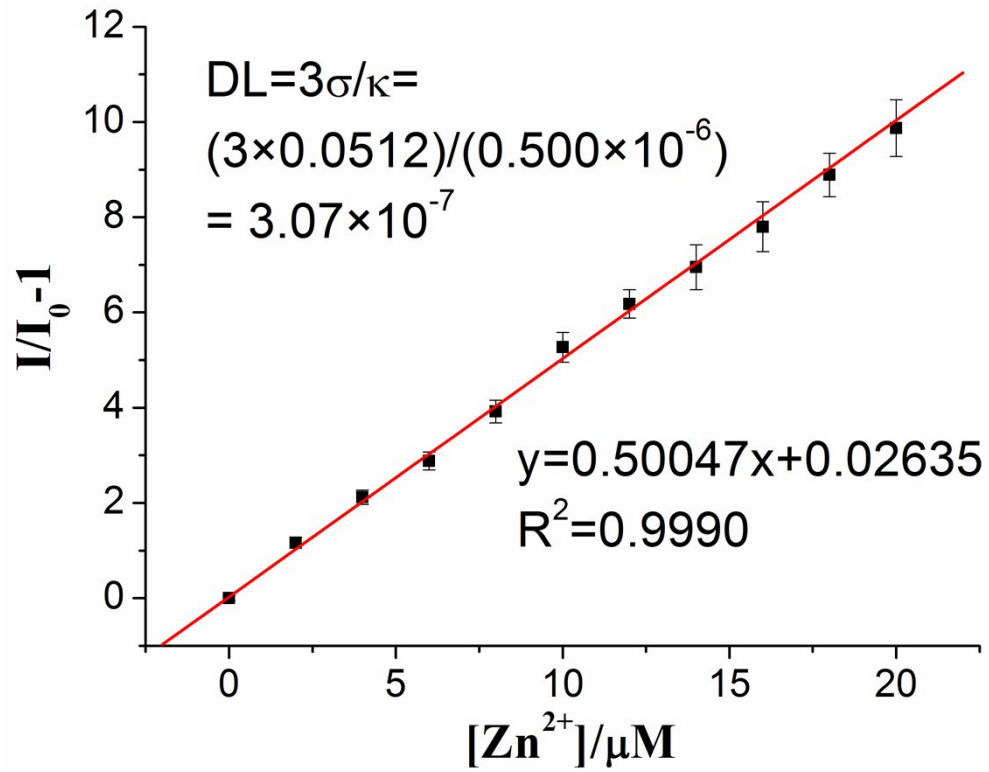

Figure S15. Linear fit equation for detection limit calculation of HL with Zn^{2+} in DMF-H_2O(v/v, 9:1) buffer solution. The detection limit was determined to be 3.07×10^{-7} M based on relative fluorescence intensity changes versus $[Zn^{2+}]$.

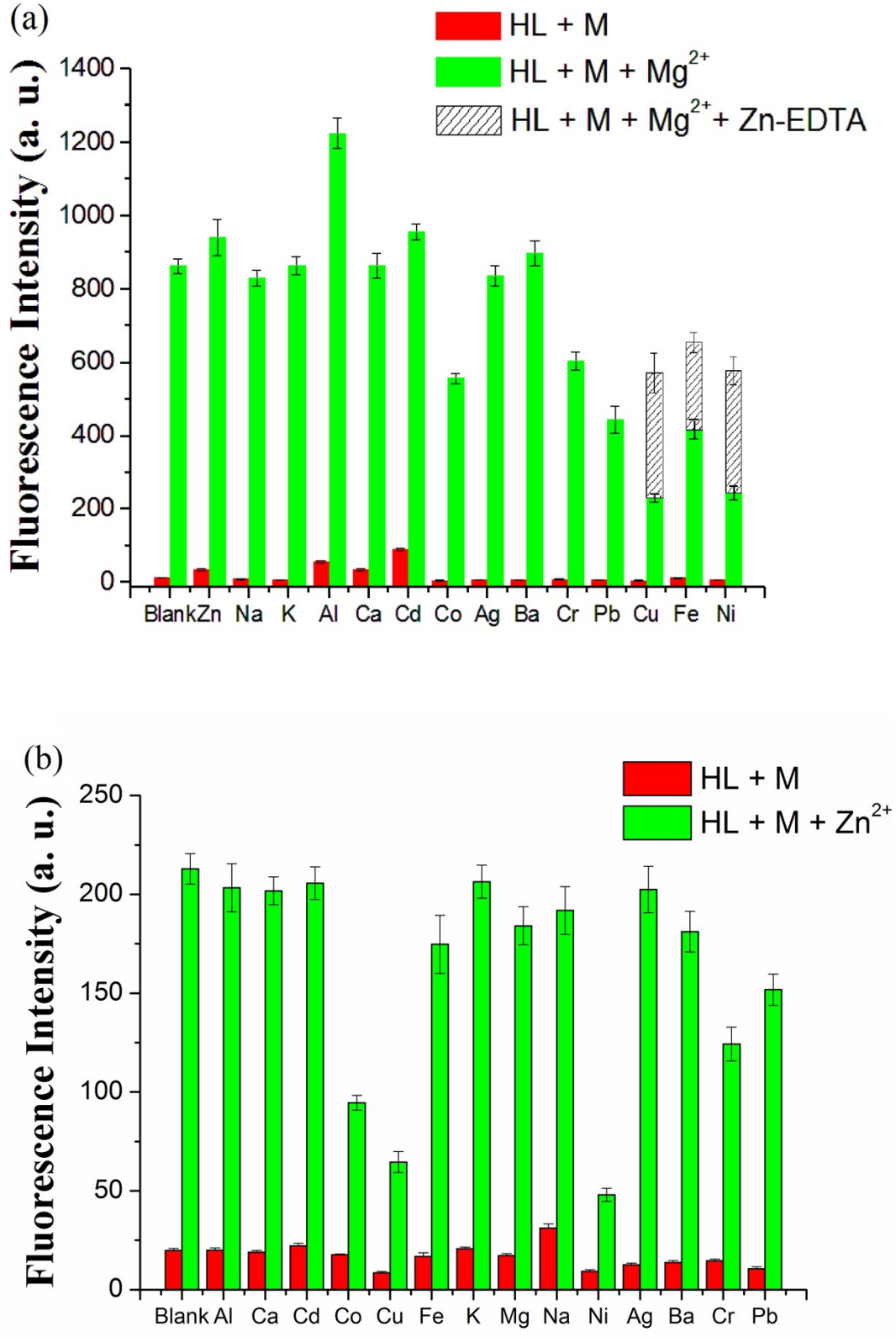

Figure S16. Fluorescence response of HL towards (a) Mg^{2+} in acetonitrile and (b) Zn^{2+} in DMF- H_2O buffer solution upon the addition of various metal ions. The red bars represent the fluorescence intensities of HL in the presence of various metal ions.

The green bars represent the changes in the fluorescence intensities that occur upon the subsequent addition of 1 equiv. of Mg^{2+} or Zn^{2+} to the HL-metal cation solutions. The three bars with the slash represents the treatment of the interfere ions with Zn^{2+}-EDTA.

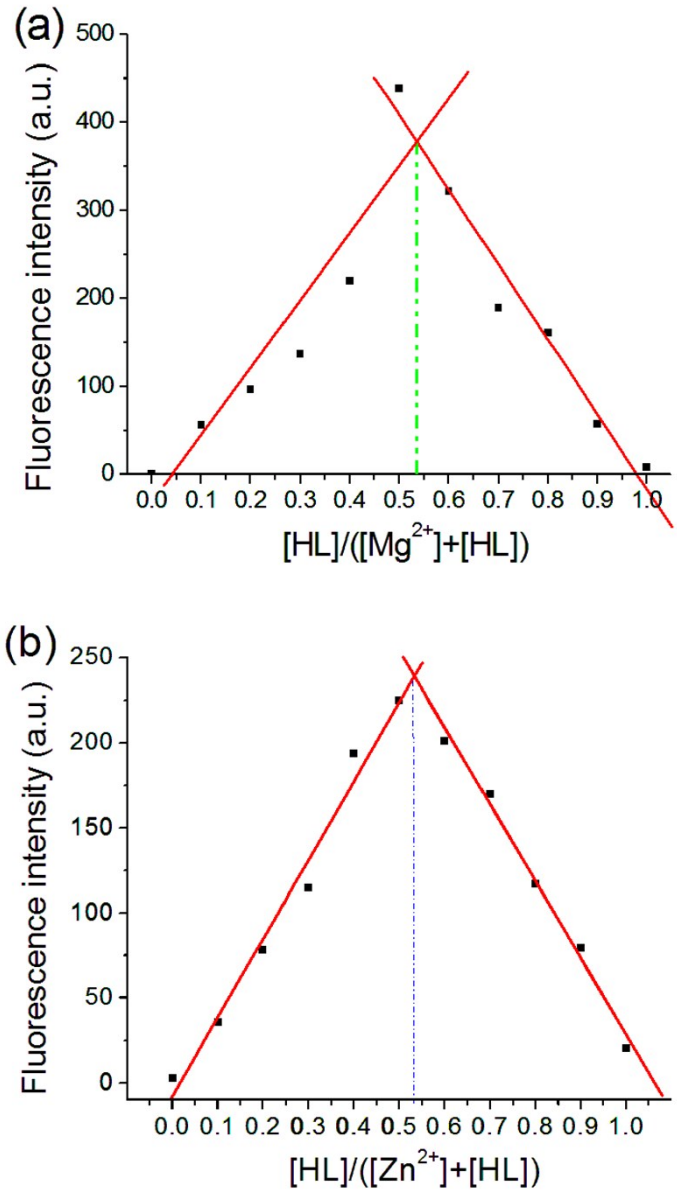

Figure S17. Job plot for the determination of the stoichiometry of HL with (a) Mg^{2+} and (b) Zn^{2+}in the complexation. Fluorescence intensity (Mg^{2+}: λ_{ex} = 350 nm; Zn^{2+}: λ_{ex} = 460 nm) was plotted as a function of the molar ratio of [HL]/([M^{2+}]+[HL])

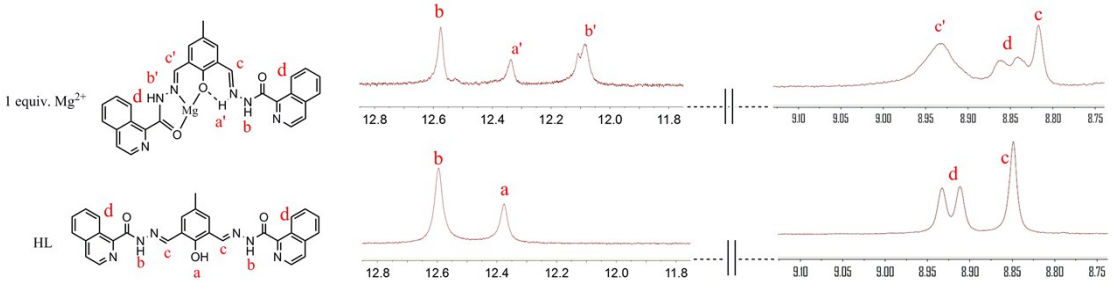

Figure S18. The ^{1}H-NMR spectra of HL upon the addition of 1 equiv. of Mg^{2+} in DMSO-d^{6}.

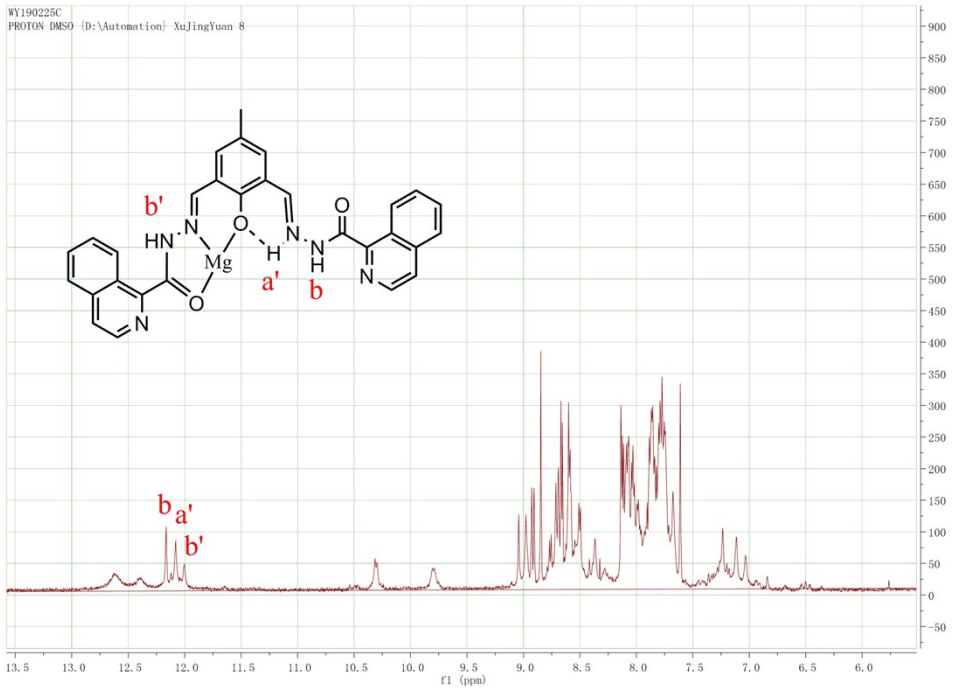

Figure S19. The ^{1}H-NMR spectra of HL upon the addition of excess $Mg(NO_3)_2$ (2.5 equiv.) in DMSO-d^{6}.

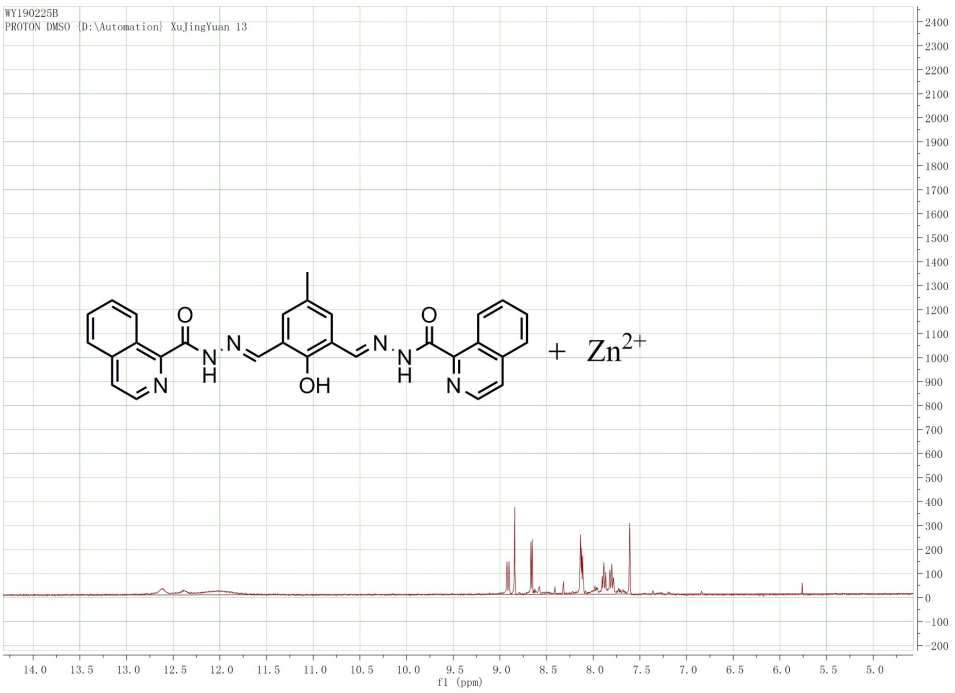

Figure S20. The ^{1}H-NMR spectra of HL upon the addition of excess $Zn(NO_3)_2$ (2.5 equiv.) in DMSO-*d*^{6}.

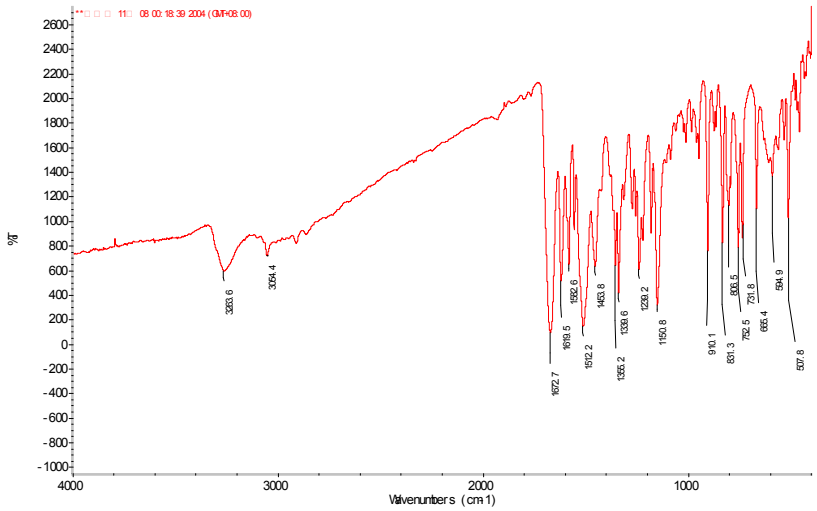

Figure S21. IR Spectrum of HL

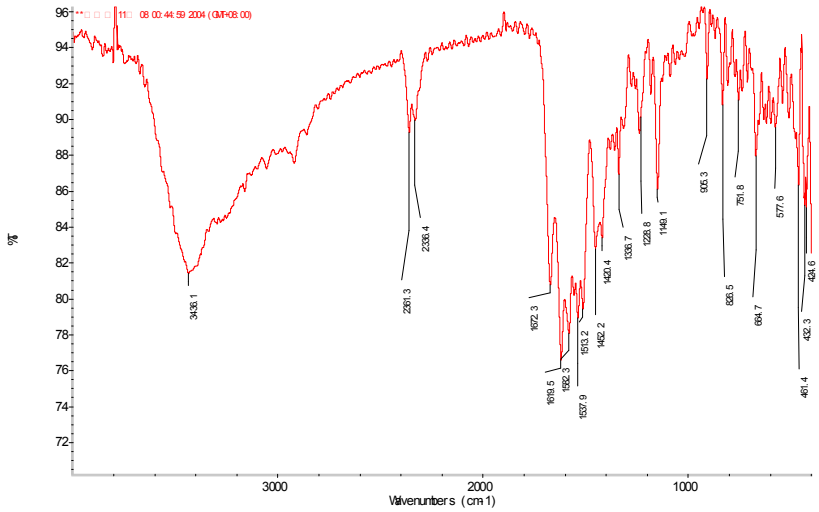

Figure S22. IR Spectrum of Mg^{2+} complex of HL

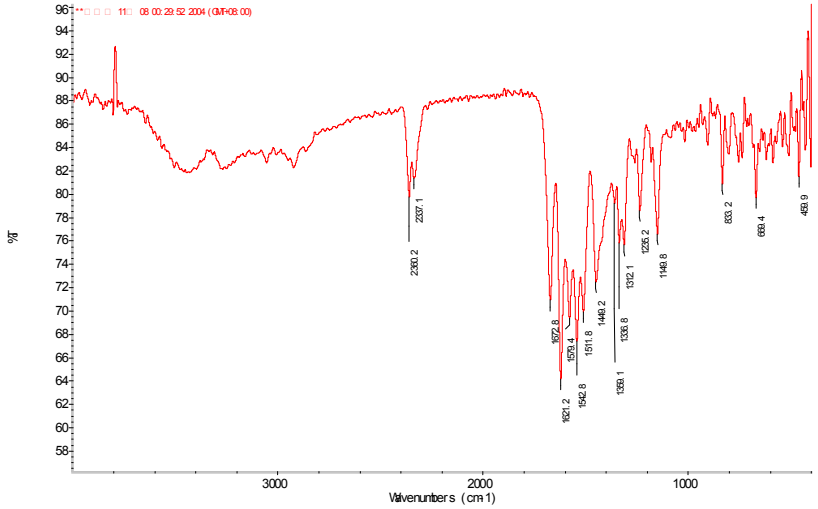

Figure S23. IR Spectrum of Zn^{2+} complex of HL

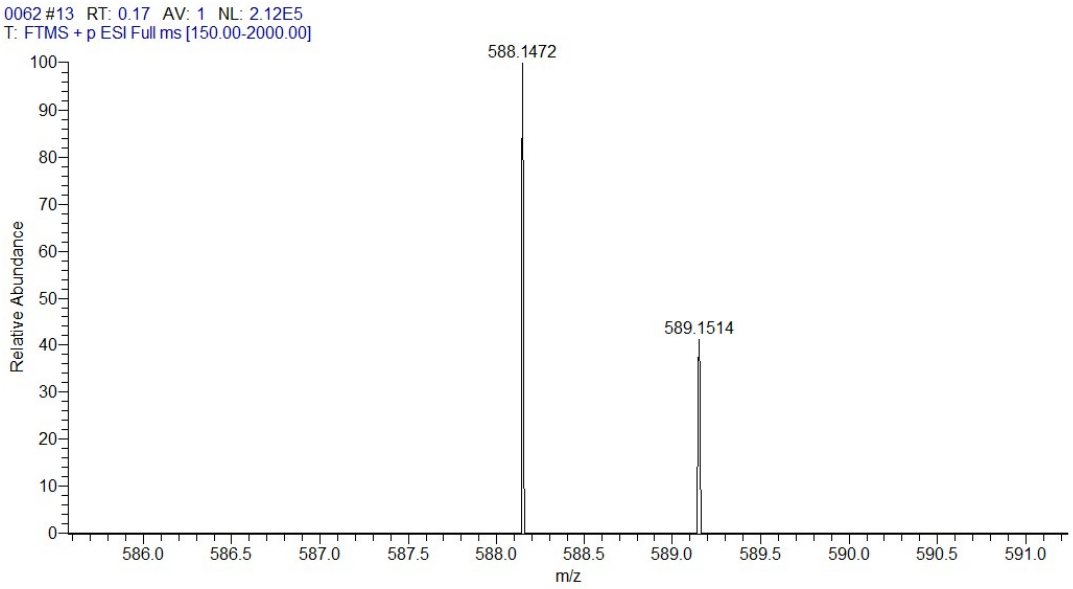

Figure S24. ESI-MS (positive mode) spectrum of HL upon addition 1 equiv of $Mg(NO_3)_2$.

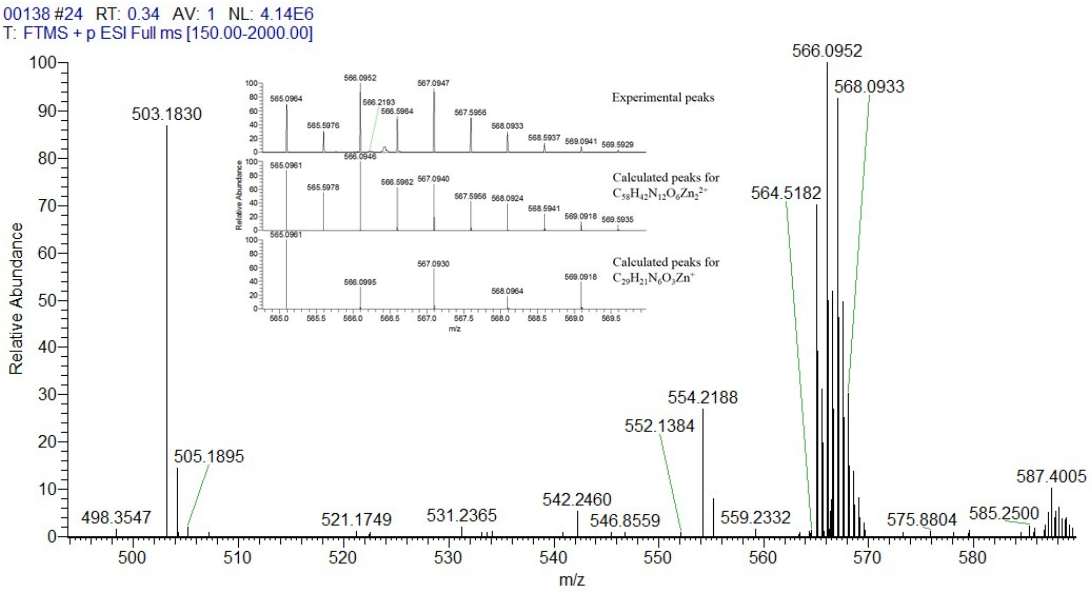

Figure S25. ESI-MS (positive mode) spectrum of HL upon addition 1 equiv of $Zn(NO_3)_2$.

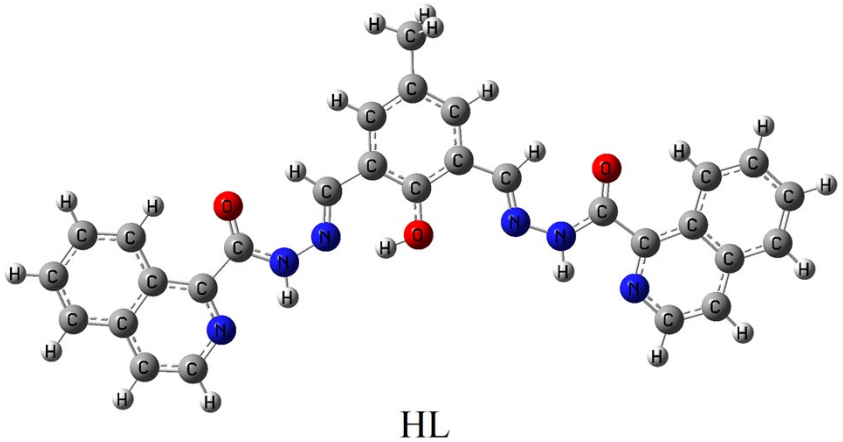

HL

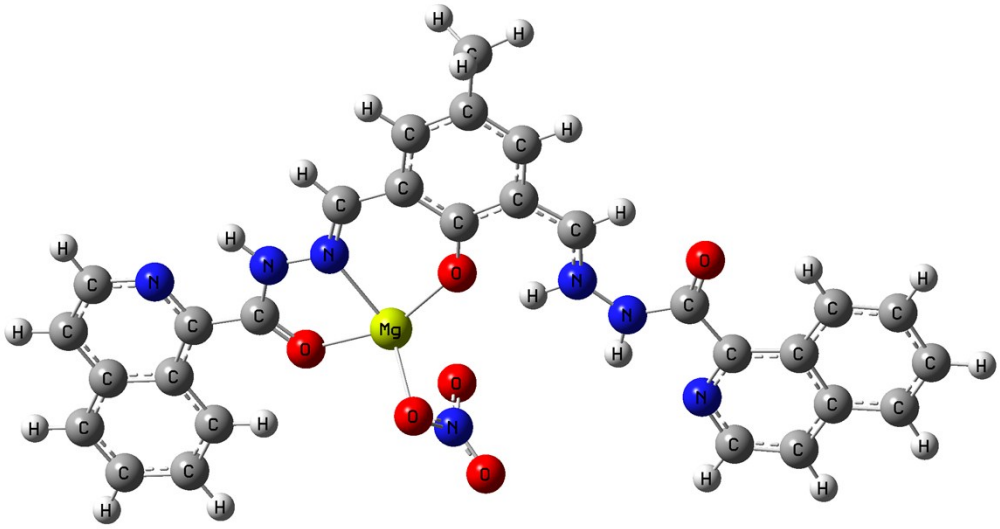

$Mg(HL)(NO_3)$

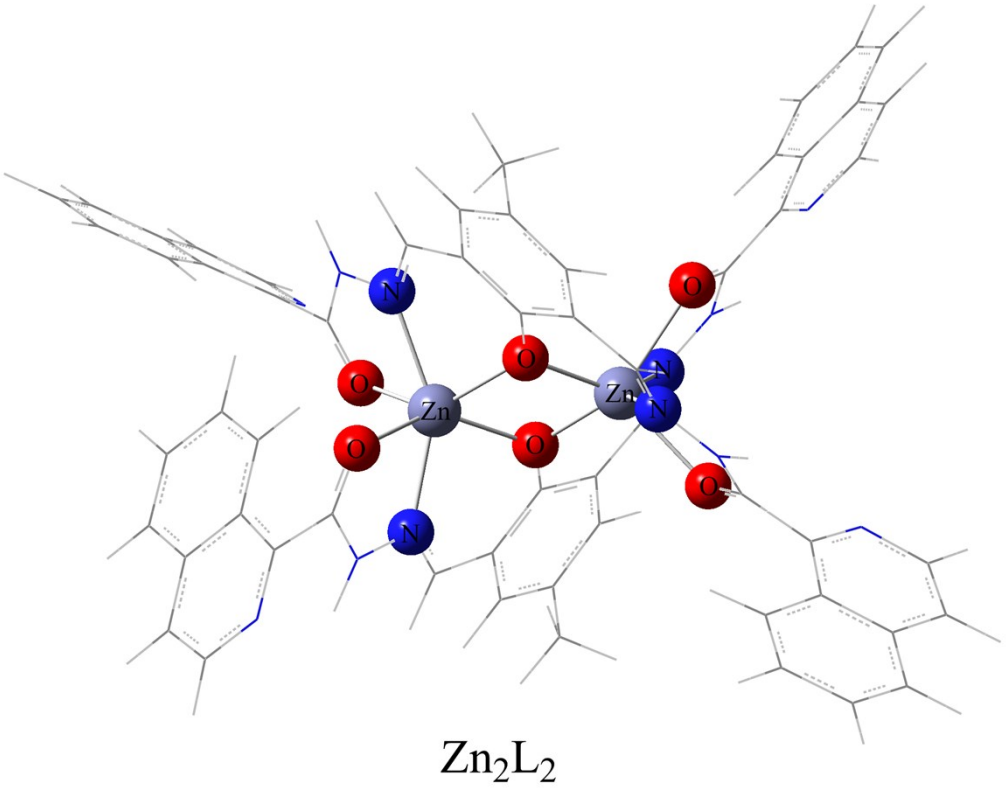

Figure S26. Optimized structures of HL and its Mg and Zn complexes.

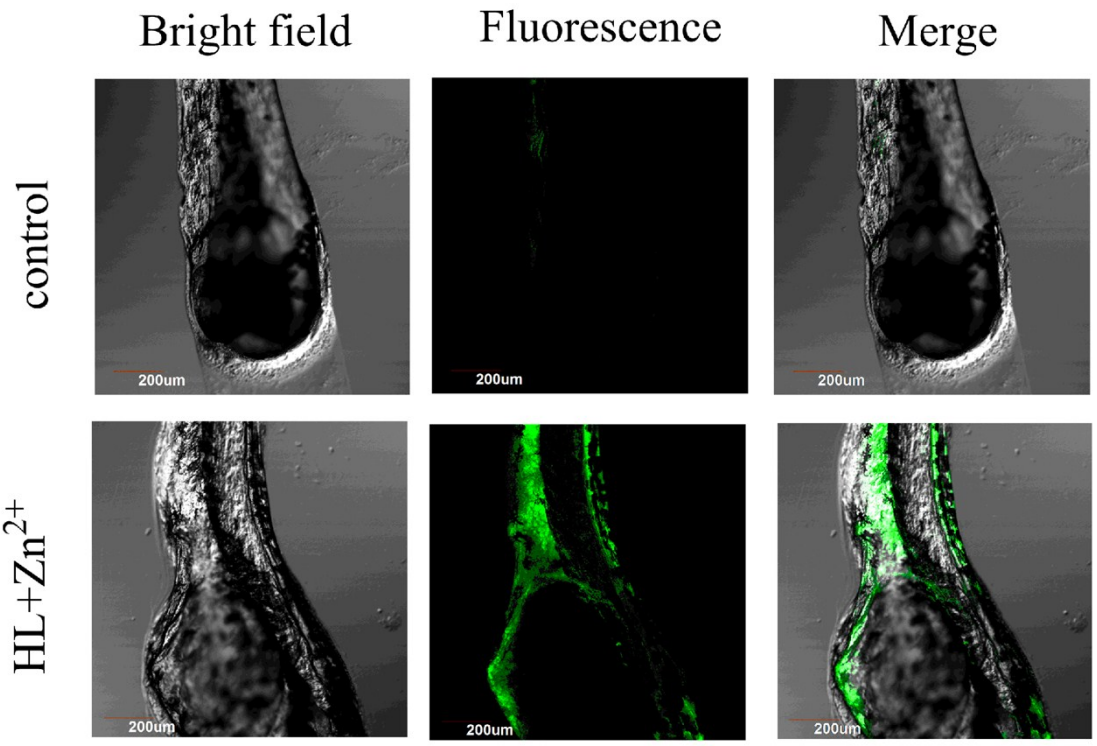

Figure S27. Confocal fluorescence images of zebrafish larvae treated with HL and zinc ions. Bright field image (left), fluorescence image (middle), and merged image (right). The scale bar is 200 □μm. □λ_{ex} = 405 nm.